Novel Superstructure of Nondiscoid Mesogens: Uneven-Parallel Association of Half-Disk Molecules, 3,4,5-Trialkoxybenzoic Anhydrides, to a Columnar Structure and Its One-Directionally Geared Interdigitation

Keiki Kishikawa,*,[†] Shigetaka Furusawa,[†] Takahiro Yamaki,[†] Shigeo Kohmoto,[†] Makoto Yamamoto,[†] and Kentaro Yamaguchi[‡]

Contribution from the Department of Materials Technology, Faculty of Engineering, Chiba University, 1-33 Yayoi-cho, Inage-ku, Chiba 263-8522, Japan, and Chemical Analysis Center, Chiba University, 1-33 Yayoi-cho, Inage-ku, Chiba 263-8522, Japan

Received September 10, 2001

Abstract: Compact and simple nondiscoid mesogens, trialkoxybenzoic anhydrides **2**−**11** ((RO)$_3$C$_6$H$_2$−CO−O−CO−C$_6$H$_2$(OR)$_3$, R = C$_2$H$_5$, n-C$_3$H$_7$, n-C$_4$H$_9$, n-C$_6$H$_{13}$, n-C$_8$H$_{17}$, n-C$_{10}$H$_{21}$, n-C$_{12}$H$_{25}$, n-C$_{14}$H$_{29}$, n-C$_{16}$H$_{33}$, and (*S*)- and (*R*)-3,7-dimethyloctyl) were designed and synthesized, and their superstructures were investigated by polarized light microscopy, differential scanning calorimetry, calculation (MM2 and AM1), circular dichroism spectroscopy, and X-ray diffraction. As the result, in the cases of **5**−**9** and **11**, the half-disk molecules in the liquid crystal phases were self-assembled by the dipole−dipole interaction between their carbonyl groups to a column in which the molecules were piled up in an alternately antiparallel manner, and the columns were interdigitated each other. The observed interdigitations were highly directional in the perpendicular direction to the column axis. In the case of compound **11** which has (*S*)- or (*R*)-3,7-dimethyloctyl groups, a helical organization of the molecules in the column was estimated from the peaks in the circular dichroism spectra. This is the first report of a one-directionally interdigitated columnar phase, and these compounds are the first liquid crystalline acid anhydrides. It was demonstrated that a −CO−O−CO− moiety is useful as a polar junction in liquid crystalline compounds.

Introduction

Columnar liquid crystal phases in which molecules are self-assembled to a columnar superstructure are useful in building nanostructures,[1] and the unique physical properties of these materials are known .[2−5] After the discovery of columnar phases in 1977,[6] discoid mesogens (hexasubstituted benzenes,[7] triphenylenes,[8] dibenzopyrenes,[9] perylenes,[10] porphyrins,[11] phthalocyanines[12]) were thought to be essential for generation of columnar mesophases. Later, however, it was found that several nondiscoid compounds generated the columnar mesophases, such as polycatenar (phasmids),[13] tetrahedral,[14] and star-shaped[15] mesogens. Then, association of half-disk shaped metallomesogens to a columnar structure by the strong attractive interaction between their metal atoms or metal oxides was reported.[16] Further, association of amide mesogens[17] and diisobutylsilanediol[18] by hydrogen bonding in the direction of the column axis and self-assembly of plural molecules into a full-disk shaped

[†] Department of Materials Technology, Faculty of Engineering.
[‡] Chemical Analysis Center.

(1) Nano structure using columnar phases: (a) Reppy, M. A.; Gray, D. H.; Pindzola, B. A.; Smithers, J. L.; Gin, D. L. *J. Am. Chem. Soc.* **2001**, *123*, 363. (b) Yeardley, D. J. P.; Ungar, G.; Percec, V.; Holerca, M. N.; Johansson, G. *J. Am. Chem. Soc.* **2000**, *122*, 1684. (c) Engelkamp, H.; Midelbeek, S.; Nolte, R. J. M. *Science* **1999**, *284*, 785. (d) Percec, V.; Ahn, C.-H.; Bera, T. K.; Ungar, G.; Yeardley, D. J. P. *Chem. Eur. J.* **1999**, *5*, 1070. (e) Braun, P. V.; Osenar, P.; Tohver, V.; Kennedy, S. B.; Stupp, S. I. *J. Am. Chem. Soc.* **1999**, *121*, 9498. (f) Lee, M.; Lee, D.-W.; Cho, B.-K.; Yoon, J.-Y.; Zin, W.-C. *J. Am. Chem. Soc.* **1998**, *120*, 13258. (g) Deng, H.; Gin, D. L.; Smith, R. C. *J. Am. Chem. Soc.* **1998**, *120*, 3522. (h) Percec, V.; Johansson, G.; Ungar, G.; Zhou, J. *J. Am. Chem. Soc.* **1996**, *118*, 9855 (i) Mukkamala, R.; Burns, C. L., Jr.; Catchings, R. M., III; Weiss, R. G. *J. Am. Chem. Soc.* **1996**, *118*, 9498.
(2) Charge transport: (a) Simmerer, J.; Glüsen, B.; Paulus, W.; Kettner, A.; Schuhmacher, P.; Adam, D.; Etzbach, K. H.; Siemensmeyer, K.; Wendorff, J. H.; Ringsdorf, H.; Haarer, D. *Adv. Mater.* **1996**, *8*, 815. (b) Van de Craats, A. M.; Warman, J. M.; De Haas, M. P.; Adam, D.; Simmrer, J.; Haarer, D.; Schumacher, P. *Adv. Mater.* **1996**, *8*, 823. (c) Boden, N.; Bushby, R. J.; Cammidge, A. N.; Clements, J.; Luo, R. *Mol. Cryst. Liq. Cryst.* **1995**, *261*, 251. (d) Arikainen, E. O.; Boden, N.; Bushby, R. J.; Clements, J.; Movaghar, B.; Wood, A. *J. Mater. Chem.* **1995**, *5*, 2161. (e) Boden, N.; Bushby, R. J.; Clements, J.; Movaghar, B.; Fonobsn, K. J.; Kreouzis, T. *Phys. Rev. B: Condens. Matter* **1995**, *52*, 13274. (f) Adam, D.; Schuhmacher, P.; Simmerer, J.; Haussling, L.; Siemensmeyer, K.; Etzbach, K. H.; Ringsdorf, H.; Haarer, D. *Nature* **1994**, *371*, 141.
(3) Fluorescence: Bayer, A.; Hübner, J.; Kopitzke, J.; Oestreich, M.; Rühle, W.; Wendorff, J. H. *J. Phys. Chem. B* **2001**, *105*, 4596.
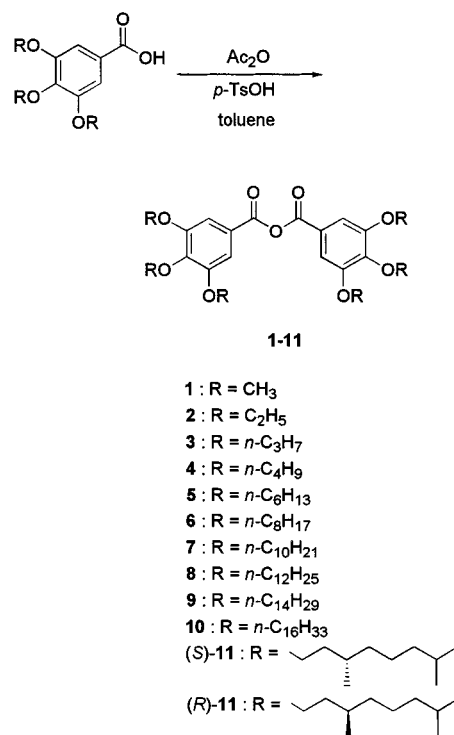
(4) Charge-transfer complex: Goldmann, D.; Janietz, D.; Schmidt, C.; Wendorff, J. H. *Angew. Chem., Int. Ed.* **2000**, *39*, 1851.
(5) Redox system: Deschenaux, R.; Schweissguth, M.; Vilches, M.-T.; Levelut, A.-M.; Hautot, D.; Long, G. J.; Luneau, D. *Organometallics* **1999**, *18*, 5553.
(6) Discovery of columnar phase: Chandrasekhar, S.; Sadashiva, B. K.; Suresh, K. A. *Pramana* **1977**, *9*, 471.
(7) Hexasubstituted benzene: (a) Maliniak, A.; Greenbaum, S.; Poupko, R.; Zimmermann, H.; Luz, Z. *J. Phys. Chem.* **1993**, *97*, 4832. (b) Tabushi, I.; Yamamura, K.; Okada, Y. *J. Org. Chem.* **1987**, *52*, 2502. (c) Chandrasekhar, S.; Sadashiva, B. K.; Suresh, K. A.; Madhusudana, N. V.; Kumar, S.; Shashidhar, R.; Venkatesh, G. *J. Phys. Colloq.* **1979**, C120.
(8) Triphenylene: (a) Boden, N.; Borner, R. C.; Bushby, R. J.; Cammidge, A. N.; Jesudason, M. V. *Liq. Cryst.* **1993**, *15*, 851. (b) Destrade, C.; Tinh, N. H.; Gasparoux, H.; Malthête, J.; Levelut, A. M. *Mol. Cryst. Liq. Cryst.* **1981**, *71*, 111. (c) Destrade, C.; Mondon, M. C.; Malthête, J. *J. Phys. Colloq.* **1979**, *C3*, 17−21.
(9) Dibenzopyrene: (a) Henderson, P.; Ringsdorf, H.; Schuhmacher, P. *Liq. Cryst.* **1995**, *18*, 191. (b) Bock, H.; Helfrich, W. *Liq. Cryst.* **1992**, *12*, 697.
(10) Perylene: Goltner, C.; Pressner, D.; Mullen, K.; Spiess, H. W. *Angew. Chem., Int. Ed. Engl.* **1993**, *32*, 1660.

supramolecule by hydrogen bonding[19] have also been reported. In the organization of the nondiscoid mesogens to the column or assembly of the nondiscoid molecules to the discoid supramolecule, strong intermolecular attractive interactions (strong arene−arene interactions in the case of the long-rod and star-shaped molecules, and metal−metal (or metal−oxygen) interactions, or hydrogen bonding in the case of small molecules) were necessary to generate the stable columnar liquid crystal phase. Recently, a weak interaction, a dipole−dipole interaction, was utilized for antiparallel organization of bent-rod molecules in columnar phases.[20,21] However, in the case of the long bent-rod molecules, four benzene and one thiophene ring with two acetylene units and two highly polar groups (cyano groups) were necessary to obtain the stable columnar mesophases.

We planned a small, simple, and basic mesogen to generate the superstructure in a mesophase with weak interactions. In our design, two benzene rings were connected with a CO−O−CO moiety which generates a larger dipole than the usual polar junctions (ester, ether, or imine). It was expected that the dipole−dipole interaction would organize the molecules with antiparallel correlation to produce a columnar structure. Simplification of mesogens also has the advantage of analyzing the superstructure of columns in the mesophase. So far, the superstructure has not been investigated in detail though packing structures of the molecules in the column are well studied. In most cases, these columns are explained by using simple cylindrical models.[22] Recently, in columnar phases of hexaalkoxy-triphenylenes which have three short and three long alkyl

Scheme 1. Synthesis of Benzoic Acid Anhydride Derivatives **1−11**

1 : R = CH$_3$
2 : R = C$_2$H$_5$
3 : R = *n*-C$_3$H$_7$
4 : R = *n*-C$_4$H$_9$
5 : R = *n*-C$_6$H$_{13}$
6 : R = *n*-C$_8$H$_{17}$
7 : R = *n*-C$_{10}$H$_{21}$
8 : R = *n*-C$_{12}$H$_{25}$
9 : R = *n*-C$_{14}$H$_{29}$
10 : R = *n*-C$_{16}$H$_{33}$
(*S*)-**11** : R =
(*R*)-**11** : R =

chains alternately, the interdigitation was observed to be less than the averaged diameters.[23] However, directionality of the interdigitation has not been reported.

In this paper, we describe a novel superstructure in mesophase, which has the following features: (1) uneven-parallel association of half-disk shaped molecules, 3,4,5-trialkoxybenzoic anhydrides, (2) one-directionally geared interdigitation of the columns, (3) association of small molecules which have a central large dipole moment, (4) a simple liquid crystalline compound which is easily available from ethyl gallate in three steps, and (5) the first mesomorphic acid anhydrides.
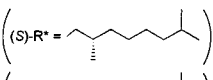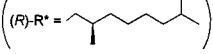
Results and Discussion

Synthesis of the Acid Anhydrides. Compound **1** is commercially available.[24] Compounds **2−11** were synthesized as follows (Scheme 1). Alkylation of ethyl gallate with 1-bromoalkanes in acetone followed by hydrolysis with KOH in water−ethanol gave the corresponding 3,4,5-trialkoxybenzoic acids. The benzoic acids were reacted with acetic anhydride in toluene in the presence of catalytic amounts of *p*-toluenesulfonic acid to obtain benzoic anhydride derivatives **2−11**, which were purified by conventional silica gel column chromatography. All the compounds were stable under atmospheric conditions. Nucleophilic attack of water molecules to the carbonyl-carbon atoms might be suppressed by π-conjugation of the carbonyl group with the electron rich aromatic ring.

Study in Polarized Light Microscopy and DSC. Behaviors of compounds **1−11** are shown in Table 1. Compounds **1−4** (R = CH$_3$, C$_2$H$_5$, *n*-C$_3$H$_7$, *n*-C$_4$H$_9$) and **10** (R = *n*-C$_{16}$H$_{33}$) did not show any mesophase. On the other hand, compounds **5−9** (R = *n*-C$_6$H$_{13}$, *n*-C$_8$H$_{17}$, *n*-C$_{10}$H$_{21}$, *n*-C$_{12}$H$_{25}$, *n*-C$_{14}$H$_{29}$) and (*S*)-

(11) Porphyrin: (a) Lelj, F.; Morelli, G.; Ricciardi, G.; Roviello, A.; Sirigu, A. *Liq. Cryst.* **1992**, *12*, 941. (b) Shimizu, Y.; Miya, M.; Nagata, A.; Ohta, K.; Matsumura, A.; Yamamoto, I.; Kusabayashi, S. *Chem. Lett.* **1991**, 25. (c) Gregg, B. A.; Fox, M. A.; Bard, A. J. *J. Chem. Soc. Chem. Commun.* **1987**, 1134.

(12) Phthalocyanines: (a) Piechocki; Engel, M. K.; Bassoul, P.; Bosio, L.; Lehmann, H.; Hanack, M.; Simon, J. *Liq. Cryst.* **1993**, 709C. (b) Van der Pol, J. F.; Neeleman, E.; Zwikker, J. W.; Nolte, R. J. M.; Drenth, W.; Aerts, J.; Visser, R.; Picken, S. J. *Liq. Cryst.* **1989**, *6*, 577. (c) Simon, J.; Skoulios, A.; Guillon, D.; Weber, P. *J. Am. Chem. Soc.* **1982**, *104*, 5245. (d) Pawlowski; Hanack, M. *Synthesis* **1980**, 287.

(13) Polycanenar: (a) Malthête, J.; Nguyen, H. T. *Liq. Cryst.* **1993**, *13*, 171. (b) Malthête, J.; Levelut, A.-M.; Nguyen, H. T. *J. Phys. Lett. (Paris)* **1985**, *46*, L-875. (c) Destrade, C.; Foucher, P.; Gasparoux, H.; Nguyen, H. T.; Levelut, A.-M.; Malthête, J. *Mol. Cryst. Liq. Cryst.* **1984**, *106*, 121.

(14) Tetrahedral mesogen: (a) Pegenau, A.; Hegmann, T.; Tschierske, C.; Diele, S. *Chem. Eur. J.* **1999**, *5*, 1643. (b) Douce, L.; El-ghayoury, A.; Skoulios, A.; Ziessel, R. *Chem. Commun.* **1999**, 2033.

(15) Star-shape mesogen: Kim, B. G.; Kim, S.; Park, S. Y. *Tetrahedron. Lett.* **2001**, *42*, 2697.

(16) Half-disk metallomesogens: (a) Trzaska, S. T.; Swager, T. M. *Chem. Mater.* **1998**, *10*, 438. (b) Zheng, H.; Xu, B.; Swager, T. M. *Chem. Mater.* **1996**, *8*, 907. (c) Zheng, H.; Lai, C. K.; Swager, T. M. *Chem. Mater.* **1995**, *7*, 2067. (d) Serrette, A. G.; Lai, C. K.; Swager, T. M. *Chem. Mater.* **1994**, *6*, 2252. (e) Lai, C. K.; Serrette, A. G.; Swager, T. M. *J. Am. Chem. Soc.* **1992**, *114*, 7948.

(17) Association of plural molecules to a discotogen by hydrogen bonding: (a) Suárez, M.; Lehn, J.-M.; Zimmerman, S. C.; Skoulios, A.; Heinrich, B. *J. Am. Chem. Soc.* **1998**, *120*, 9526. (b) Kleppinger, R.; Lillya, C. P.; Yang, C. *J. Am. Chem. Soc.* **1997**, *119*, 4097. (c) Kleppinger, R.; Lillya, C. P.; Yang, C. *Angew. Chem., Int.Ed. Engl.* **1995**, *34*, 1637.

(18) Isobutylsilanediol: Bunning, J. D.; Lydon, J. E.; Eaborn, C.; Jackson, P. H.; Goodby, J. W.; Gray, G. W. *J. Chem. Soc., Faraday Trans. 1* **1982**, 713.

(19) Benzamides: (a) Percec, V.; Ahn, C.-H.; Bera, T. K.; Ungar, G.; Yeardley, D. J. P. *Chem. Eur. J.* **1999**, *5*, 1070. (b) Malthête, J.; Levelut, A.-M.; Libert, L. *Adv. Mater.* **1992**, *4*, 37. (c) Kobayashi, Y.; Matsunaga, Y. *Bull. Chem. Soc. Jpn.* **1987**, *60*, 3515. (d) Matsunaga, Y.; Terada, M. *Mol. Cryst. Liq. Cryst.* **1986**, *141*, 321.

(20) Bent-rod molecules with a central large dipole: Kishikawa, K.; Harris, M. C.; Swager, T. M. *Chem. Mater.* **1999**, *11*, 867.

(21) Columnar phase of bent-rod molecules with a central large dipole: Levitsky, I. A.; Kishikawa, K.; Eichhorn, S. H.; Swager, T. M. *J. Am. Chem. Soc.* **2000**, *122*, 2474.

(22) Chandrasekhar, S. In *Handbook of Liquid Crystals, Low Molecule Weight Liquid Crystal II*; Demus, D., Goodby, J. W., Gray, G. W., Spiess, H.-W., Vill, V., Eds.; Wiley-VCH: New York, 1998; Chapter 8 (Columnar, Discotic Nematic and Lamellar Liquid Crystals: Their Structures and Physical Properties).

(23) Allen, M. T.; Harris, K. D. M.; Kariuki, B. M.; Kumari, N.; Preece, J. A.; Diele, S.; Lose, D.; Hegmann, T.; Tschierske, C. *Liq. Cryst.* **2000**, *27*, 689.

(24) Compound **1** was purchased from Tokyo Chemical Industry Co., Ltd.

Table 1. Phase Behavior of Compounds **1**–**11**[a]

Compound	Behavior
1 : R = CH$_3$	K$_1$ —141 (0.1)→ K$_2$ —160 (9.8) / 142 (-9.6)— I
2 : R = C$_2$H$_5$	K$_1$ ⇌74 (h$_1$) / 44 (-6.2)→ K$_2$ —80 (h$_2$)→ I (h$_1$+h$_2$=7.9)[b]
3 : R = C$_3$H$_5$	K ⇌77 (4.2) / 69 (-4.1)⇌ I
4 : R = C$_4$H$_9$	K$_1$ —17 (1.1)→ K$_2$ —79 (3.6) / 70 (-3.7)— I
5 : R = C$_6$H$_{13}$	Col ⇌64 (2.1) / 61 (-1.8)⇌ I
6 : R = C$_8$H$_{17}$	K —33 (16.3)→ Col —62 (2.1) / 59 (-2.1)— I
7 : R = C$_{10}$H$_{21}$	K —15 (3.6)→ Col —61 (2.4) / 56 (-2.1)— I
8 : R = C$_{12}$H$_{25}$	K$_1$ ⇌17 (7.3) / 13 (-7.6)⇌ K$_2$ —27 (3.3)→ Col —49 (1.5) / 45 (-1.4)— I
9 : R = C$_{14}$H$_{29}$	K$_1$ ⇌32 (5.9) / 26 (-0.3)⇌ K$_2$ —38 (9.9) / 35 (-10.0)— Col ⇌52 (1.8) / 49 (-1.7)⇌ I
10 : R = C$_{16}$H$_{33}$	K$_1$ ⇌55 (29.8) / 32 (-9.1)⇌ K$_2$ —72 (33.1) / 47 (-14.4)— I
(*S*)-**11** : R = (*S*)-R*	Col ⇌33 (2.5) / 30 (-1.9)⇌ I (*S*)-R* =
(*R*)-**11** : R = (*R*)-R*	Col ⇌34 (2.3) / 30 (-1.9)⇌ I (*R*)-R* =

[a] The transition temperatures (°C) and enthalpies (in parentheses, kcal/mol) were determined by DSC (5°/min) and are given above and below the arrows. K, K$_1$, and K$_2$ indicate crystal phases and Col indicates a columnar phase, respectively. [b] The sum of enthalpies h$_1$ and h$_2$ was measured because the peaks could not be separated.

Figure 1. Textures of the liquid crystals in polarized light microscopy (×400): (a) compound **6** at 40 °C, (b) **8** at 31 °C.

and (*R*)-**11** (R = (*S*)- and (*R*)-3,7-dimethyloctyl) showed enantiotropic columnar liquid crystal phases. Oily compound **5** showed a columnar liquid crystal phase up to 64 °C on heating, and its crystallization was not detected by differential scanning calorimetry (DSC) carried out to 0 °C. Compounds **6**–**9** showed crystal-to-liquid crystalline phase transitions, respectively. Compounds (*S*)- and (*R*)-**11** showed columnar phases and their transition temperatures from the liquid crystal to the liquid were lower than the others. In polarized light microscopy, typical textures of columnar phases were observed for all the liquid crystalline compounds. It was confirmed that the molecules did not tilt with respect to the column axis because the extinction brushes of the circular domains exactly agreed with the directions of the polarizer and analyzer of the microscope in all the columnar phases[25] (Figure 1, a and b). Textures of **8** (Figure 1b) and **9** were slightly different than those of **5**–**7**. Compounds **5**–**7** showed smooth surfaces of the focal conics. In the textures of compounds **8** and **9**, the focal conics had many lines and their surfaces were uneven. In the DSC study, enthalpies of **5**, **6**, and **7** in the liquid crystalline-to-liquid-phase transitions were about 2 kcal/mol, and those of **8** and **9** were 1.4–1.8 kcal/mol. Transition enthalpy of **11** (1.9–2.5 kcal/mol) was the largest one in this series. The difference in the enthalpies may originate in the difference in tightness of packing of the columns.

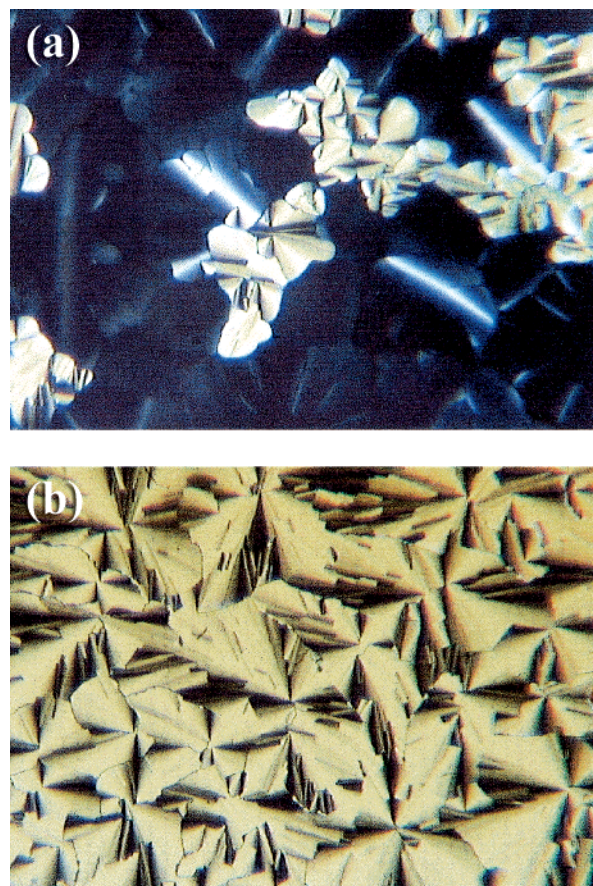**Study of Powder X-ray Diffraction.** Though compounds **3** and **4** did not show any liquid crystal phase and were solid at

(25) Frank, F. C.; Chandrasekhar, S. *J. Phys. (France)* **1980**, *41*, 1285.

room temperature, their peak patterns in powder X-ray diffraction (XRD) were similar to those of columnar phases which have large peaks at the small angle region (**3**, $d = 14.5$; **4**, $d = 16.0$ and 16.4 Å, respectively) and a halo in the large angle region. This indicates that these compounds also have columnar structures and the molecules are highly disordered by vibration of the aromatic rings and movement of the alkyl chains even in the crystal phases. XRD data of the liquid crystalline compounds are shown in Table 2. All the liquid crystal phases showed complicated charts which have several broad peaks in their small angle region. The mesophase of **5** was a rectangular columnar phase. The mesophases of **6** and **7** were classified into oblique columnar phases and the peak positions were almost constant in the temperature range (40–60 °C), respectively. Though **8** and **9** also showed oblique phases, different diffraction patterns from those of **5**–**7** were observed. Considerably large broad peaks were observed at 4.1–4.2, 8.4–8.5, and 12.5 Å in the case of **8** and at 3.8, 4.1, and 8.7 Å in the case of **9**. This indicates that the molecules in those columns are more ordered in the direction of the column axis than the others, and the multiple distances (4.1–4.2, 8.4–8.7, and 12.5 Å) correspond to once, twice, and three times the molecular thickness, respectively. The peak at 3.8 Å in the XRD of **9** corresponds to the thickness of the aromatic ring. The peak patterns in the small angle region were also different from the others, in which the large peaks were observed in two areas, 36.2–36.8 and 26.3–22.3 Å in the case of **8** and 52.6 and 24.8–26.6 Å in the case of **9**. The XRD data of (*S*)-**11** showed five peaks in the small angle region (24.2–21.1 Å) and the distance (4.7 Å) of

Table 2. XRD Data for the Liquid Crystal Phases of Compounds **5**–**9** and **11**

compound	temp, °C	phase[a]	parameter	d	(calcd d)	Miller index	a/b
5: R = C$_6$H$_{13}$	20	Col$r$	a = 37.4	18.7	(18.7)	(200)	1.90
			b = 19.7	17.4	(17.4)	(110)	
				4.2			
	30	Col$r$	a = 37.8	18.9	(18.9)	(200)	1.96
			b = 19.3	17.2	(17.2)	(110)	
				4.3			
	40	Col$r$	a = 37.4	18.7	(18.7)	(200)	1.89
			b = 19.8	17.5	(17.5)	(110)	
				4.3			
	50	Col$r$	a = 37.0	18.5	(18.5)	(200)	1.88
			b = 19.7	17.4	(17.4)	(110)	
				4.3			
	60	Col$r$	a = 39.2	19.6	(19.6)	(200)	1.93
			b = 20.3 and	18.0	(18.0)	(110)	
			a = 37.0	18.5	(18.5)	(200)	1.91
			b = 19.4	17.2	(17.2)	(110)	
				4.3			
6: R = C$_8$H$_{17}$	40	Colob	a = 44.7	22.3	(22.3)	(200)	1.98
			b = 22.6	21.0	(20.8)	(1−10)	
			θ = 94.5	19.7	(19.6)	(110)	
				4.4			
	50	Colob	a = 44.7	22.3	(22.3)	(200)	1.98
			b = 22.6	21.0	(20.8)	(1−10)	
			θ = 94.5	19.7	(19.6)	(110)	
				4.4			
	60	Colob	a = 44.7	22.3	(22.3)	(200)	1.92
			b = 23.3	21.2	(21.1)	(1−10)	
			θ = 93.0	20.3	(20.2)	(110)	
				4.4			
7: R = C$_{10}$H$_{21}$	40	Colob	a = 51.8	25.7	(25.7)	(200)	1.99
			b = 26.0	24.3	(24.5)	(1−10)	
			θ = 97.1	22.0	(22.2)	(110)	
				4.3			
	50	Colob	a = 51.6	25.7	(25.7)	(200)	1.95
			b = 26.5	24.3	(24.5)	(1−10)	
			θ = 95.5	22.5	(22.7)	(110)	
				4.3			
	60	Colob	a = 51.6	25.7	(25.7)	(200)	1.97
			b = 26.2	24.0	(24.1)	(1−10)	
			θ = 94.6	22.5	(22.6)	(110)	
				4.3			
8: R = C$_{12}$H$_{25}$	30	Colob	a = 74.3	36.8	(36.8)	(200)	2.94
			b = 25.3	24.8	(25.0)	(1−10)	
			θ = 97.9	22.8	(23.0)	(110)	
				12.5			
				8.4			
				4.1			
	40	Colob	a = 75.1	36.8	(36.8)	(200)	2.97
			b = 25.3	25.2	(25.6)	(1−10)	
			θ = 101.5	22.3	(22.6)	(110)	
				12.5			
				8.5			
				4.3			
	50	Colob	a = 73.3	36.2	(36.2)	(200)	2.90
			b = 25.3	25.1	(25.2)	(1−10)	
			θ = 99.3	22.7	(22.8)	(110)	
				12.5			
				8.5			
				4.3			
9: R = C$_{14}$H$_{29}$	40	Colob	a = 109.7	52.6	(52.6)	(200)	3.55
			b = 30.9	26.6	(26.6)	(1−10)	
			θ = 106.7	24.8	(24.8)	(110)	
				14.6			
				8.7			
				4.1			
				3.8			
11: R = (S)-3,7-dimethyloctyl	20	Col$r$	a = 48.0	24.0	(24.0)	(200)	1.83
			b = 26.2	23.0	(23.0)	(110)	
				4.7			
	27	Col$r$ and	a = 48.4	24.2	(24.2)	(200)	1.86
			b = 26.0	22.9	(22.9)	(110)	
		Colob	a = 47.3	23.6	(23.6)	(200)	1.92
			b = 24.6	22.4	(22.5)	(1−10)	
			θ = 95.8	21.1	(21.2)	(110)	
				4.7			

[a] Col$r$ and Colob indicate rectanguler columnar and oblique columnar phases, respectively.
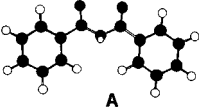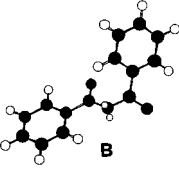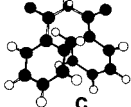
the broad peak in the large angle region was 0.5 Å longer than those of the others, which originates in the bulkiness of the 3-methyl groups of the alkyl chains. The ratios of a/b were 1.83–1.99 in the case of **5**–**7** and **11**. The ratios were larger than that of hexagonal columnar phases ($a/b \simeq 1.73$). The angle θ increased with an increase of the alkyl chain length.

Compounds **8** and **9** showed larger a/b ratios (**8**, a/b = 2.90–2.97; **9**, a/b = 3.55) than the others.

Conformational Study by MM2 and AM1 Calculations. To estimate the most stable conformation of the benzoic anhydride derivatives, energies of benzoic anhydride conformers **A**, **B**, and **C** which equilibrate each other in rotational isomer-

Table 3. Calculation of Conformers of Benzoic Anhydride

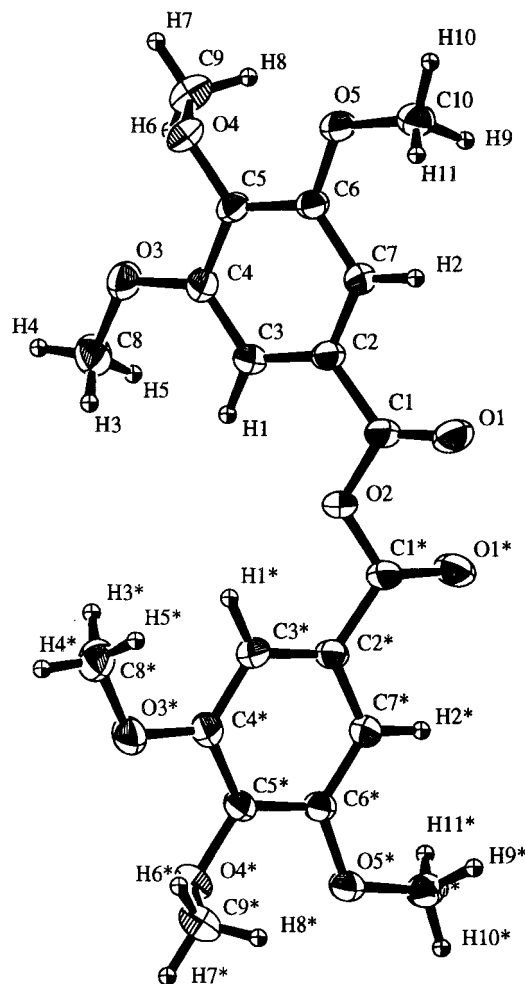|	relative energy (kcal/mol)	
	MM2 [a]	AM1 [b]
A	0.0	0.0
B	0.5	2.4
C	4.4	6.2

[a] Reference 26. [b] Reference 27.

ization around the two C−O single bonds were calculated by two methods, MM2[26] and AM1[27] (Table 3). Both methods indicated that conformer **A** was the most stable one. The difference in these stabilities depends on electrostatic repulsion between the carbonyl-oxygen atoms and the lone pair electrons of the central oxygen atom. In conformer **A**, the two carbonyl-oxygen atoms are on the opposite side to the lone pair electrons, while in conformers **B** and **C** the lone pairs are on the same side with one and two of the carbonyl oxygen-atoms, respectively. Accordingly, the frequency of conformer **A** was supposed to be greater than that of **B** or **C** in the liquid crystal phase.

Single-Crystal X-ray Diffraction. To investigate the conformation of the trialkoxybenzoic anhydrides in the crystal phase, single-crystal X-ray crystallography was performed. Although **4** (R = n-C$_4$H$_9$) gave clear single crystals which were large enough for the measurement, no diffraction peaks were observed at $2\theta = 20-30°$. On the other hand, a single crystal of **1** (R = CH$_3$) gave clear diffraction peaks and the structure was solved (Figure 2). The two carbonyl groups point the same direction, and each carbonyl group and its neighboring aromatic ring are in the same plane. The conformation of **1** in the crystalline state is similar to that of conformer **A** which was calculated as one molecule in a vacuum. Accordingly, it is most probable that compound **1** adopts a conformation similar to that of conformer A in the liquid crystal phase.

Calculation of Net Atomic Charges and a Dipole Moment. Net atomic charges and a dipole moment of benzoic anhydride were calculated by AM1 for conformer **A** (Scheme 2). The two carbonyl-carbon atoms are highly positive (+0.37) and the three oxygen atoms are highly negative (−0.29 and −0.32). The molecule has a large dipole moment at its center (5.0 D). From these results, it was estimated that the molecules in the liquid crystal phase were organized by the intermolecular dipole−dipole interaction. Antiparallel association of the molecules is the most effective arrangement to cancel their dipoles. If the

(26) The MM2 calculation was carried out by a molecular modeling software, Chem3D (Cambridge software corporation).
(27) AM1 calculation was carried out by a software, WinMOPAC Ver.3 (Fujitsu, Ltd.). Stewart, J. J. P. *J. Comput. Chem.* **1989**, *10*, 209−220 and 221−264.

Figure 2. X-ray structure of **1**. ORTEPs shown at 30% probability.

Scheme 2. Net Atomic Charges and Dipole Moment of Benzoic Anhydride Calculated by AM1
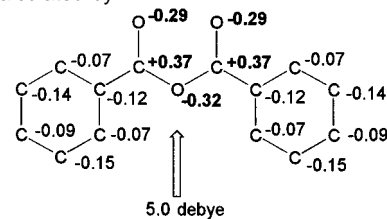

O=C−O−C=O moieties closely contact each other in an antiparallel manner to obtain the maximum attractive interaction, the molecules appear to be piled up successively in an alternately antiparallel manner to form a column.

Interdigitation of Columns in the Mesophase. In Table 2, the ratios a/b were 1.83−1.99 in the cases of **5**−**7** and **11**. Those ratios were larger than that of a hexagonal columnar phase ($a/b \simeq 1.73$), which could be explained by diminution of the lattice parameter b due to 1) a tilt of the molecules in the column, or 2) an interdigitation between the columns.

If the diminution of lattice parameter b is explained only by a tilt of the molecules in the column, the tilt angle should be about 45° which is calculated from arccosine of (column diameter)/(molecular width). However, the large tilt angle is not suitable for stability of the liquid crystal phase, because a tilt of the disk-shaped supramolecules makes the cross section of the column oval, which suppresses rotation of each column

Scheme 3. Compounds **12a** and **12b**

12a (R = *n*-C$_8$H$_{17}$)
12b (R = *n*-C$_{12}$H$_{25}$)
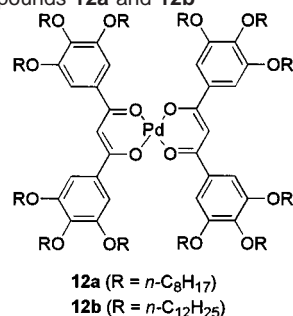
around the column axis. Further, the alternately antiparallel
piling up of the molecules makes spaces between the molecules,
and it is assumed that interdigitation is necessary to fill those
spaces. Moreover, the tilt was not observed in the extinction
brushes of the textures in polarized light microscopy.

The diminution of lattice parameter *b* could be explained only
by interdigitation of the columns. If the two-half-disk molecules
associate to generate a full-disk shape, this disk-unit has twelve
alkyl chains. Bis[1,3-bis(3′,4′,5′-trioctyloxyphenyl)-1,3-propan-
dionate]palladium(II) **12a** (R = *n*-C$_8$H$_{17}$) and Bis[1,3-bis(3′,4′,5′-
tridodecoxyphenyl)-1,3-propandionate]palladium (II) **12b** (R =
n-C$_{12}$H$_{25}$) also have twelve alkyl chains around the discoid
mesogen (Scheme 3)[28] and the disk size is similar to those of
dimers of **6** (R = *n*-C$_8$H$_{17}$) and **8** (R = *n*-C$_{12}$H$_{25}$), respectively.
Parameters *a* of **12a** and **12b** in the hexagonal columnar phases
(**12a**, *a* = 30.08 Å at 66 °C; **12b**, *a* = 37.08 Å at 57 °C), which
equals the intercolumnar distances (i.e., diameters of the
columns), are longer than parameters *b* of **6** and **8** in the
columnar phases (**6**, *b* = 22.6−23.3 Å at 40−60 °C; **8**, *b* =
25.3 Å at 30−50 °C) which are nearly equal to the intercolumnar
distances in the direction of the *y* axis. Accordingly, it also can
be seen that distances between (100) planes in the hexagonal
columnar phase are diminished in the cases of **5**−**7** and **11**. In
the cases of **8** (R = *n*-C$_{12}$H$_{25}$) and **9** (R = *n*-C$_{14}$H$_{29}$), especially,
the distances between the columns are ultimately diminished
only in the direction. The rates of the diminution were 8.0−12,
9.9−12, 11−13, 40−42, and 51% for **5**, **6**, **7**, **8**, and **9**. In the
case of **9**, the diminution rate was considered to be almost the
limit of interdigitation. The rate for (*S*)-**11** (5.5−9.9%) which
has chiral and bulky alkyl chains was the smallest in this series.
The bulky alkyl chains seemed to suppress the interdigitation
between the columns.

**Estimation of Superstructures in Chiral Half-Disk Shaped
Molecules (*S*)- and (*R*)-11 from Their CD Spectra.** Circular
dichroism (CD) spectra of (*S*)-**11** and (*R*)-**11** were measured as
follows. The compounds sandwiched between two quartz plates
(the sample thickness: 4 μm) were melted by heating and were
allowed to stand at room temperature. Directors of the columns
in the liquid crystal phase were vertically aligned to the plate
surface, which was confirmed by polarized light microscopy.

In the CD spectra of **11**, two peaks (339 and 242 nm) which
belong to the n−π* and π−π* transitions, respectively, were
observed (Figure 3). In the case of (*S*)-**11**, a peak at 339 nm
was positive and one at 242 nm was negative. On the other
hand, (*R*)-**11** showed opposite signs to the peaks of (*S*)-**11**. This
symmetry clarified that the CD peaks depend on an enantiomeric
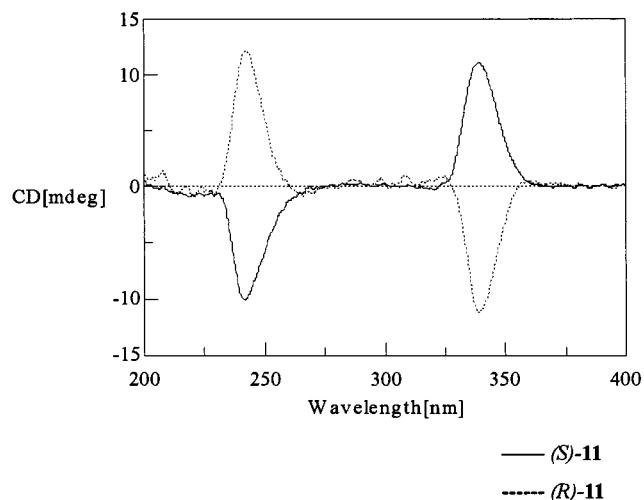relation between (*S*)- and (*R*)-**11**. Further, the chirality was

(28) Zheng, H.; Lai, C. K.; Swager, T. M. *Chem. Mater.* **1995**, *7*, 2067.

Figure 3. CD spectra of (*S*)- and (*R*)-**11**. The compounds sandwiched
between two quartz plates (the sample thickness: 4 μm) were melted by
heating and were allowed to stand at room temperature. Directors of the
columns in the liquid crystal phase were vertically aligned to the plate
surface, which was confirmed by polarized light microscopy.

Scheme 4. Schematic Representation of Self-Assembly of the
Molecules
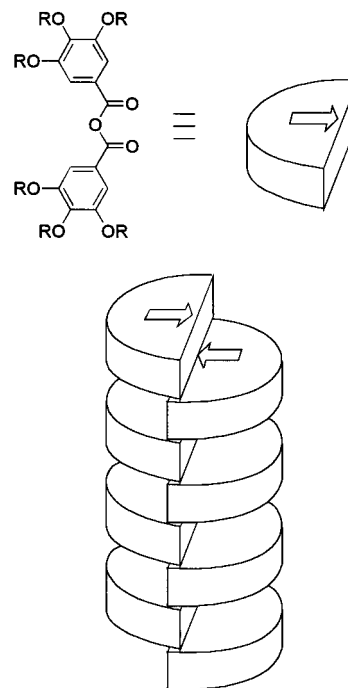
supposed to originate in the superstructure in the liquid crystal
phase, because any CD band was not observed in a solution of
(*S*)-**11** in *n*-hexane (4.0 × 10^{-5} M, path length = 10 mm). From
MOS-F (INDO/S) calculation[29] of trimethoxybenzoic anhydride
in the most stable conformation, large transition moments were
found at 347 and 337 nm (3.5 and 3.4 D), and 264, 258, 223,
and 222 nm (4.0, 3.6, 3.6, and 4.1 D) (Scheme 6 (1)). The
direction of the electric transition in the n−π* transitions (347
and 337 nm) is opposite to the one in the π−π* transitions
(264, 258, 223, and 222 nm). In the n−π* transition, transitions
a and *b* of the two-half-disk molecules overlap in an antiparallel
manner, which is depicted as a portion of a *P* helical column
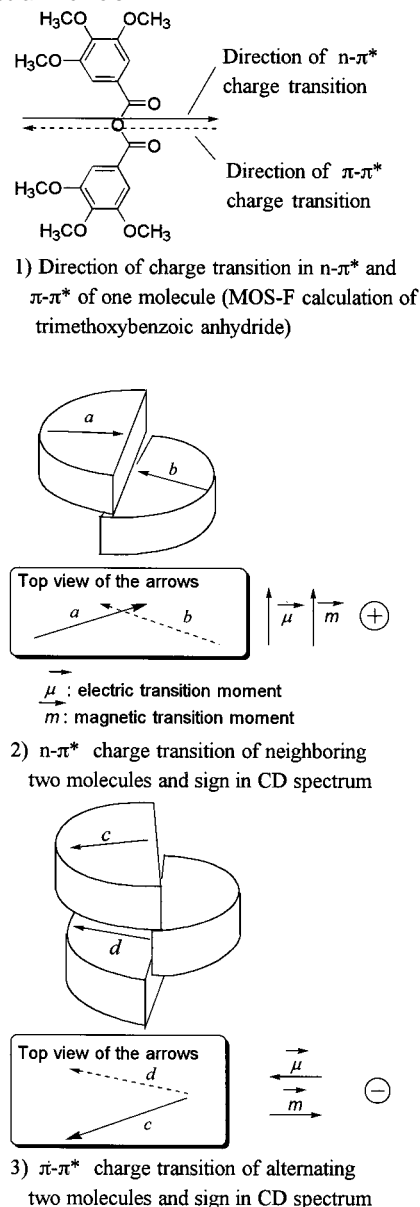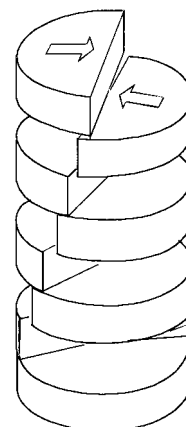
(29) MOS-F calculation program in WinMOPAC 3.0: Matsuura, A. MOS-F
4.2C, Fujitsu Ltd: Tokyo, Japan, 2000.

Scheme 5. Schematic Representation of Maximum and Minimum Overlappings of the Two Columns

1) Maximum overlapping of two columns

2) Minimum overlapping of two columns
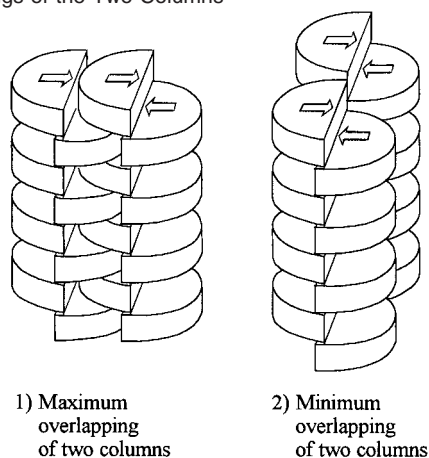
(Scheme 6 (2)). The relation of transitions *a* and *b* is important for analyzing the peak at 339 nm because lone pair electrons of the carbonyl oxygen atoms are transferred to the π^*-molecular orbital. From a top view of the arrows *a* and *b*, the electric and magnetic transition moments are parallel, which gives a positive sign in the CD spectrum.[30] The sign agreed with the observed positive sign of (*S*)-**11** at 339 nm. Movements of π-electrons of the benzene rings are important to analyze the CD spectrum of the $\pi-\pi^*$ transition. So we focused on transition moments *c* and *d* of the alternating two molecules (Scheme 6 (3)), because their benzene rings are close to each other. The three molecules are also depicted as one part of a *P* helical column. From the top view of arrows *c* and *d*, the electronic and magnetic moments are antiparallel, which gives a negative sign in the CD spectrum. It also agreed with the negative sign of (*S*)-**11** at 242 nm.

From these CD analyses, the chiral superstructure of (*S*)-**11** was estimated to be a *P* helical organization (Scheme 7). The *P* helical organizations were also reported in superstructures of liquid crystalline molecules which had (*S*)-3-methylated alkyl chains.[1c,31] Accordingly, the steric repulsions of the chiral alkyl chains between molecules in the columnar phase of (*S*)-**11** generate the *P* chirality in the column.

Mixing Experiment of 6 and (*S*)-11. Although molecular size (width and length) of (*S*)-**11** (R = (*S*)-3,7-dimethyloctyl) nearly equals that of **6** (R = *n*-octyl), (*S*)-**11** has bulkier alkyl chains than **6**. It is expected that columnar phases of the mixtures are more stable than that of pure (*S*)-**11**, because the addition of **6** decreases the averaged intermolecular distance in the column and increases the dipole−dipole interaction between the piling molecules. The result of the mixing experiments is shown in Figure 4. Transition temperatures of the mixtures from the isotropic liquid to columnar phase on slow cooling (0.5 °C/min) were plotted against mole distributions (%) of **6** in the mixture of **6** and **11**. All the transition temperatures were above the straight dashed line which was drawn from the transition temperature at 0% to that at 100%. This indicates that these two compounds can be mixed freely in the liquid crystal phase at any distribution ratio and all the generated liquid crystal

(30) Theory of CD spectrum: Snatzke, G. *Angew. Chem., Int. Ed. Engl.* **1979**, *18*, 363.
(31) P-helical organization generated by (*S*)-3-methylated alkyl groups: (a) Fujiki, M. *J. Am. Chem. Soc.* **2000**, *122*, 3336. (b) Amabilino, D. B.; Ramos, E.; Serrano, H.-L.; Sierra, T.; Veciana, J. *J. Am. Chem. Soc.* **1998**, *120*, 9126.
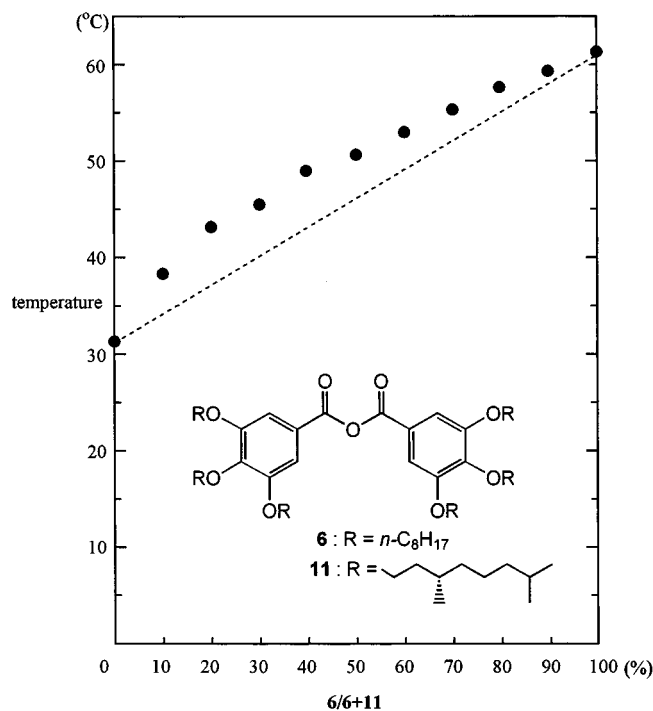
Scheme 6. Relation between Charge Transition Moments of Two Molecules, Electric and Magnetic Transition Moments, and the Sign in Circular Dichroism

1) Direction of charge transition in n-π^* and π-π^* of one molecule (MOS-F calculation of trimethoxybenzoic anhydride)

$\vec{\mu}$: electric transition moment
m: magnetic transition moment

2) n-π^* charge transition of neighboring two molecules and sign in CD spectrum

3) π-π^* charge transition of alternating two molecules and sign in CD spectrum

Scheme 7. Schematic Representation of a Chiral Columnar Structure of (*S*)-**11**

phases have higher transition temperatures than that of (*S*)-**11**. This indicates that a decrease in bulkiness of the alkyl chains

Figure 4. Plot of transition temperatures from isotropic liquid to liquid crystal against percentages of **6** in a mixture of **6** and **11**. The dots indicate the transition temperatures from isotropic liquid to liquid crystal. The straight dashed line was drawn from transition temperature at 0% to that at 100%.

shortens the averaged intermolecular distance and increases the carbonyl−carbonyl interaction.

Mechanism for Organization of the Molecules in the Columnar Phase. Schematic representation of the column is shown in Scheme 4. The antiparallel association caused by the intermolecular dipole−dipole interaction organizes the half-disk molecules to a columnar structure and the association makes spaces between the piling molecules which allow the columns to interdigitate each other. Accordingly, the large a/b ratios can be explained by the one-directionally geared interdigitation of the columns (Scheme 5). Scheme 5 represents the maximum (a) and minimum (b) overlappings of the two neighboring columns, respectively. The maximum overlapping is most suitable for high-density packing of the columns, while the minimum overlapping is not adequate for the interdigitation. The columns in all the liquid crystal phases interdigitate each other in one direction to give smaller intercolumnar distances than their column diameters, which results in the large a/b ratios. The longer alkyl chains seem to increase the intermolecular interaction of the mesogenic cores relatively, which is well-known in stabilization of smectic phases with longer alkyl-chain lengths. The stronger intercolumnar core−core interaction makes spinning of the columns around the column axis slower, which reinforces the one-directionally geared interdigitation. Hence, the ratio of a/b increases with an increase of the alkyl chain lengths. In the case of **8** and **9**, the effect seemed to be larger than that in the other cases. In the case of **11**, suppression of the interdigitation by the bulky alkyl chains seems to give the smallest a/b ratio. The mixing experiment of **6** and **11** revealed that the columns have enough flexibility and spaces to gear each other. This anisotropicity in the perpendicular direction with respect to the column axis might reflect the uneven surfaces of the textures of **8** and **9** in polarized light microscopy.

Conclusions

These results have clarified that half-disk shaped mesogens with a central large dipole in a columnar phase are organized into a column in which the molecules are piled up with an alternately antiparallel manner, and the columns interdigitate each other with gearing. The observed interdigitation was highly directional perpendicular to the column axis. To the best of our knowledge, this is the first report of a one-directionally interdigitated columnar phase. Further, in the self-assembly of the benzoic anhydride derivatives which are simple and easily available, we could demonstrate that −CO−O−CO− is useful as a polar junction in liquid crystalline compounds. The geared column structure in the self-assembly can be assumed to be a useful method to generate highly ordered superstructures in materials.

Experimental Section

Materials. Toluene (Nakarai Chemical) was dried over 4A molecular sieves. Acetic anhydride and *p*-toluenesulfonic acid monohydrate (Nakarai Chemical) were used as received. Silica gel (Merck, silica gel 60) was dried with heating at 120 °C for 3 h (this procedure is important to suppress hydrolysis in column chromatograpy). Solvents for the column chromatography, ethyl acetate and hexane (Nakarai Chemical), were used as received.

General Methods. ^{1}H NMR (400 MHz) and ^{13}C NMR (126.5 MHz) spectra were recorded on JEOL LA400 and GSX500 spectrometers, respectively. CDCl$_3$ was used as solvent and TMS as internal standard. Chemical shifts are reported as δ, ppm. IR spectra were recorded on a JASCO FT/IR410 spectrometer with the sample pressed in a KBr-pellet technique. High-resolution mass spectra were performed on a JEOL JMS-HX110. Thermal transitions of samples were measured on a MAC Science DSC3100S differential scanning calorimeter (DSC). In all cases, the heating and cooling rates were 5°/min. Indium was used as a calibration standard. A Nikon ECLIPSE E400POL optical polarized microscope (×200 magnification) equipped with an INSTEC HCS400 hot stage and a Fujifilm Finepix 700 digital camera (×2 magnification) was used to verify thermal transitions and characterize anisotropic textures.

Powder X-ray diffraction (XRD) experiments were performed using a MAC Science M18XHF²²-SRA diffractometer. The samples were held in a capillary within a temperature cell controlled to within ±0.1 °C. Single X-ray diffraction was measured on a Rigaku AFC7S diffractometer with graphite-monochromated Cu Kα radiation. The structure was solved by direct method (SIR92). The non-hydrogen atoms were refined anisotropically, and the hydrogen atoms were included but not refined.

A Typical Procedure for Synthesis of Trialkoxybenzoic Anhydride (Synthesis of 9). Acetic anhydride (3.04 g, 29.8 mmol) and *p*-toluenesulfonic acid monohydrate (114 mg, 0.599 mmol) were added to a 50 mL toluene solution of 4.52 g (5.95 mmol) of 3,4,5-tritetradecoxybenzoic acid, and the mixture was refluxed for 1 h. The excess acetic anhydride and generated acetic acid were removed by distillation. The crude product was purified by silica gel chromatography (ethyl acetate−*n*-hexane, 1:30) to give **9** as a white solid (2.79 g, 62.4%).

2 (R = *n*-C$_2$H$_5$): white solid; 36.0%; IR (KBr) 2976, 1994, 1684, 1588, 1392 cm^{-1}; ^{1}H NMR (395.7 MHz, CDCl$_3$) δ 1.37 (t, 3H, J = 6.8 Hz), 1.38 (t, 3H, J = 6.8 Hz), 1.45 (t, 12H, J = 6.8 Hz), 4.10−4.20 (m, 12H), 7.35 (s, 3H); ^{13}C NMR (125.6 MHz, CDCl$_3$) δ 14.77, 14.80, 15.60, 64.77, 64.95, 69.02, 69.17, 108.73, 109.26, 123.29, 123.72, 142.90, 143.82, 152.68, 152.91, 162.36, 170.82; HRMS (FAB) calcd for C$_{26}$H$_{34}$O$_9$ (M$^+$) 490.2202, found 490.2183.

3 (R = *n*-C$_3$H$_7$): white solid; 41.0%; IR (KBr) 2940, 1785, 1705, 1390, 1120 cm^{-1}; ^{1}H NMR (395.7 MHz, CDCl$_3$) δ 1.05 (t, 6H, J =

7.4 Hz), 1.06 (t, 12H, $J = 7.4$ Hz), 1.80−1.89 (m, 12H), 4.00 (t, 8H, $J = 6.6$ Hz), 4.06 (t, 4H, $J = 6.6$ Hz), 7.35 (s, 4H); ^{13}C NMR (125.6 MHz, CDCl$_3$) δ 10.42, 10.50, 22.57, 23.21, 70.87, 75.21, 109.13, 123.19, 144.05, 153.05, 162.37; HRMS (FAB) calcd for C$_{32}$H$_{46}$O$_9$ (M$^+$) 574.3141, found 574.3122.

4 (R = n-C$_4$H$_9$): white crystal; 20.1%; IR (KBr) 2950, 1785, 1715, 1435, 1340 cm^{-1}; ^{1}H NMR (395.7 MHz, CDCl$_3$) δ 0.96 (t, 6H, $J = 3.6$ Hz), 0.99 (t, 12H, $J = 3.6$ Hz), 1.46−1.58 (m, 12H), 1.71−1.84 (m, 12H), 4.03 (t, 4H $J = 6.7$ Hz), 4.08 (t, 8H, $J = 6.7$ Hz), 7.34 (s, 4H); ^{13}C NMR (125.6 MHz, CDCl$_3$) δ 13.64, 13.69, 18.99, 19.12, 31.17, 32.21, 68.88, 73.13, 108.94, 123.11, 143.92, 153.00, 162.28; HRMS (FAB) calcd for C$_{38}$H$_{58}$O$_9$ (M$^+$) 658.4080, found 658.4022.

5 (R = n-C$_6$H$_{13}$): oil (liquid crystal); 7.4%; IR (NaCl) 2924, 1785, 1782, 1710, 1588, 1462 cm^{-1}; ^{1}H NMR (395.7 MHz, CDCl$_3$) δ 0.83 (t, 6H, $J = 3.5$ Hz), 0.84 (t, 12H, $J = 3.5$ Hz), 1.19−1.51 (m, 36H), 1.66−1.79 (m, 12H), 3.95 (t, 4H, $J = 6.3$ Hz), 4.00 (t, 8H, $J = 6.3$ Hz), 7.27 (s, 4H); ^{13}C NMR (125.6 MHz, CDCl$_3$) δ 13.89, 13.95, 22.51, 22.57, 25.59, 25.66, 29.15, 30.21, 31.46, 31.61, 69.27, 73.57, 108.99, 123.15, 143.96, 153.03, 162.35; HRMS (FAB) calcd for C$_{50}$H$_{82}$O$_9$ (M$^+$) 826.5958, found 826.5941.

6 (R = n-C$_8$H$_{17}$): white crystal; 56.0%; IR (KBr) 2930, 1785, 1715, 1590, 1435 cm^{-1}; ^{1}H NMR (395.7 MHz, CDCl$_3$) δ 0.87 (t, 6H, $J = 3.9$ Hz), 0.89 (t, 12H, $J = 3.9$ Hz), 1.28−1.58 (m, 60H), 1.72−1.85 (m, 12H), 4.01 (t, 4H $J = 6.2$ Hz), 4.01 (t, 8H, $J = 6.2$ Hz), 7.33 (s, 4H); ^{13}C NMR (125.6 MHz, CDCl$_3$) δ 14.01, 14.03, 22.60, 22.64, 25.98, 26.03, 29.22, 29.24, 29.30, 29.44, 30.30, 31.77, 31.84, 69.32, 73.63, 109.04, 123.17, 144.01, 153.06, 162.40; HRMS (FAB) calcd for C$_{62}$H$_{106}$O$_9$ (M$^+$) 994.7836, found 994.7780.

7 (R = n-C$_{10}$H$_{21}$): 19.7%; IR (NaCl) 2876, 1794, 1592, 1440, 1334, 1118 cm^{-1}; ^{1}H NMR (395.7 MHz, CDCl$_3$) δ 0.86 (t, 6H, $J = 4.0$ Hz), 0.88 (t, 12H, $J = 4.0$ Hz), 1.27−1.58 (m, 84H), 1.72−1.85 (m, 12H), 4.01 (t, 4H, $J = 6.3$ Hz), 4.01 (t, 4H, $J = 6.3$ Hz), 4.07 (t, 8H, $J = 6.3$ Hz), 7.33 (s, 4H); ^{13}C NMR (125.6 MHz, CDCl$_3$) δ 14.03, 22.63, 25.99, 26.05, 29.25, 29.31, 29.35, 29.51, 29.54, 29.59, 29.62, 29.68, 30.32, 31.87, 31.89, 69.31, 73.61, 109.02, 123.18, 144.00, 153.06, 162.37; HRMS (FAB) calcd for C$_{74}$H$_{130}$O$_9$ (M$^+$), 1162.9714, found 1162.9728.

8 (R = n-C$_{12}$H$_{25}$): 2.86%; IR (KBr) 2920, 2850, 1765, 1590, 1435, 1335 cm^{-1}; ^{1}H NMR (395.7 MHz, CDCl$_3$) δ 0.88 (t, 18H, $J = 4.9$ Hz), 1.26−1.57 (m, 108H), 1.74−1.83 (m, 12H), 4.01 (t, 4H $J = 6.0$ Hz), 4.06 (t, 8H, $J = 6.0$ Hz), 7.33 (s, 4H); ^{13}C NMR (125.6 MHz, CDCl$_3$) δ 14.06, 22.66, 26.02, 26.07, 26.18, 29.27, 29.34, 29.37, 29.49, 29.53, 29.60, 29.64, 29.68, 29.70, 30.34, 31.91, 69.33, 70.94, 73.64, 109.05, 123.19, 144.01, 153.08, 162.41; HRMS (FAB) calcd for C$_{86}$H$_{154}$O$_9$ (M$^+$), 1331.1592, found 1331.1600.

9 (R = n-C$_{14}$H$_{29}$): 62.4%; IR (KBr) 2918, 2850, 2361, 1760, 1590, 1467, 1431 cm^{-1}; ^{1}H NMR (395.7 MHz, CDCl$_3$) δ 0.88 (t, 18H, $J = 6.1$ Hz), 1.26−1.58 (m, 132H), 1.74−1.83 (m, 12H), 4.01 (t, 8H, $J = 6.5$ Hz), 4.07 (t, 4H, $J = 6.5$ Hz), 7.33 (s, 4H); ^{13}C NMR (125.6 MHz, CDCl$_3$) δ 14.12, 22.71, 26.07, 26.12, 29.32, 29.40, 29.44, 29.59, 29.67, 29.70, 29.74, 30.39, 31.97, 69.41, 73.72, 109.12, 123.24, 144.09, 153.14, 162.47; HRMS (FAB) calcd for C$_{98}$H$_{179}$O$_9$ (MH$^+$) 1500.3550, found 1500.3505.

10 (R = n-C$_{16}$H$_{33}$): 36.0%; IR (KBr) 2912, 2848, 1758, 1722, 1588, 1466, 1432 cm^{-1}; ^{1}H NMR (395.7 MHz, CDCl$_3$) δ 0.88 (t, 18H, $J = 5.9$ Hz), 1.26−1.58 (m, 156H), 1.72−1.85 (m, 12H), 4.01 (t, 4H, $J = 6.5$ Hz), 4.06 (t, 8H, $J = 6.5$ Hz), 7.33 (s, 4H); ^{13}C NMR (125.6 MHz, CDCl$_3$) δ 14.11, 22.69, 26.04, 26.09, 29.27, 29.37, 29.41, 29.56, 29.65, 29.68, 29.72, 30.35, 31.93, 69.31, 73.67, 108.97, 123.17, 143.94, 153.07, 162.43; HRMS (FAB) calcd for C$_{110}$H$_{203}$O$_9$ (MH$^+$) 1668.5428, found 1668.5360.

11 (R = (S)- and (R)-3,7-dimethyloctyl): 21.8% and 44.4%; IR (NaCl) 2930, 2370, 1785, 1715, 1595, 1435 cm^{-1}; ^{1}H NMR (395.7 MHz, CDCl$_3$) δ 0.86 (d, 12H, $J = 6.5$ Hz), 0.87 (d, 36H, $J = 6.5$ Hz), 0.93 (d, 6H, $J = 6.5$ Hz), 0.94 (d, 12H, $J = 6.5$ Hz), 1.14−1.34 (m, 24H), 1.49−1.64 (m, 12H), 1.71 (m, 6H), 1.80−1.92 (m, 6H), 4.01−4.15 (m, 12H), 7.35 (s, 4H); ^{13}C NMR (125.6 MHz, CDCl$_3$) δ 19.52, 22.54, 22.57, 22.65, 24.67, 24.69, 27.93, 29.60, 29.78, 36.26, 37.30, 37.43, 39.20, 39.31, 67.62, 71.86, 109.02, 123.20, 144.01, 153.09, 162.51; HRMS (FAB) calcd for C$_{74}$H$_{130}$O$_9$ (M$^+$) 1162.9714, found 1162.9712; (S)-form [α]$^{27}_D$ = −2.7° ($c = 1.2 \times 10^{-2}$ g/mL, n-hexane, cell length; 100 mm) for 96% ee; (R)-form α^{29}_D = +2.9° ($c = 1.2 \times 10^{-2}$ g/mL, n-hexane cell length; 100 mm) for 97% ee.

X-ray Crystal Structure Determination of 1. Single crystals were obtained by slow isothermal evaporation of a solution of **1** in a chloroform/n-hexane (1:1) mixture. The crystal measured was a colorless prism and the dimension was $0.69 \times 0.40 \times 0.30$ mm. The crystal was set on a glass fiber.

Crystal Data of 1. C$_{20}$H$_{22}$O$_9$, $M = 406.39$, prismatic, orthorhombic, $a = 4.6728(9)$, $b = 14.553(2)$, and $c = 29.643(1)$ Å, $U = 2015.7(4)$ Å^3, $T = 298$ K, space group *Pbcn* (No. 60), $Z = 4$, $D_{calc} = 1.339$ g/cm^3, μ(Cu Kα) = 9.05 cm^{-1}, 2261 reflections measured, 1596 reflections used in all calculations. The final R, wR, and GOF were 0.057, 0.073, and 2.90.

CD Spectroscopy of 11. The sample was sandwiched between two quartz plates (the sample thickness: 4 μm), melted by heating, and allowed to stand at room temperature. In the liquid crystal phase at room temperature, vertical alignment of the columns was confirmed by polarized light microscopy. The CD spectra of (S)- and (R)-**11** from 200 to 500 nm were measured at 25 °C to give two peaks, respectively. The CD spectrum of (S)-**11** in n-hexane (4.0×10^{-5} M, path length = 10 mm at 25 °C) was also measured, but no peak was observed.

Mixing Experiment of 6 and (S)-11. A chloroform solution of **6** (1.00×10^{-4} M, 20 mL) and a chloroform solution of (S)-**11** (1.00×10^{-4} M, 20 mL) were prepared. The two solutions were mixed with various ratios (1.00:9.00, 2.00:8.00, 3.00:7.00, 4.00:6.00, 5.00:5.00, 6.00:4.00, 7.00:3.00, 8.00:2.00, 9.00:1.00) using a 10 mL-measuring pipet and the solvent was evaporated in a vacuum. Transition temperatures of the nine mixtures were measured by a polarized light microscope equipped with a hot stage, respectively (temperature rate: 0.5°/min)

Supporting Information Available: X-ray structure report of **1** and charts of powder X-ray diffraction of **5**, **6**, **7**, **8**, **9**, and (S)-**11** (PDF). These materials are available free of charge via the Internet at http://pubs.acs.org.

JA012156K